











## RESEARCH LETTER

10.1029/2023GL106183

# Regime-Dependence of Nocturnal Nitrate Formation via $N_2O_5$ Hydrolysis and Its Implication for Mitigating Nitrate Pollution

### Key Points:

- Nocturnal  $pNO_3^-$  formation via  $N_2O_5$  hydrolysis is dependent on the regime defined by the ratio of  $NO_2$  to  $O_3$
- Nocturnal  $pNO_3^-$  formation via  $N_2O_5$  hydrolysis in the residual layer over megacity Beijing is more efficient than at ground level
- Nocturnal  $pNO_3^-$  formation via  $N_2O_5$  hydrolysis is suppressed in an  $O_3$ -limited regime but enhanced in a  $NO_2$ -limited regime

Pengkun Ma<sup>1</sup>, Jiannong Quan<sup>1</sup> , Youjun Dou<sup>1</sup>, Yubing Pan<sup>1</sup>, Zhiheng Liao<sup>1</sup>, Zhigang Cheng<sup>1</sup>, Xingcan Jia<sup>1</sup> , Qianqian Wang<sup>1</sup>, Junlei Zhan<sup>2</sup>, Wei Ma<sup>2</sup>, Feixue Zheng<sup>2</sup>, Yuzheng Wang<sup>2</sup>, Yusheng Zhang<sup>2</sup>, Chenjie Hua<sup>2</sup>, Chao Yan<sup>2,3</sup>, Markku Kulmala<sup>2,4</sup> , Yangang Liu<sup>5</sup> , Xin Huang<sup>3</sup> , Bin Yuan<sup>6</sup> , Steven S. Brown<sup>7</sup> , and Yongchun Liu<sup>2</sup> 

<sup>1</sup>Institute of Urban Meteorology, Chinese Meteorological Administration, Beijing, China, <sup>2</sup>Aerosol and Haze Laboratory, Advanced Innovation Center for Soft Matter Science and Engineering, Beijing University of Chemical Technology, Beijing, China, <sup>3</sup>Joint International Research Laboratory of Atmospheric and Earth System Sciences, School of Atmospheric Sciences, Nanjing University, Nanjing, China, <sup>4</sup>Faculty of Science, Institute for Atmospheric and Earth System Research, University of Helsinki, Helsinki, Finland, <sup>5</sup>Environmental and Climate Sciences Department, Brookhaven National Laboratory, Upton, NY, USA, <sup>6</sup>Institute for Environmental and Climate Research, Jinan University, Guangzhou, China, <sup>7</sup>Chemical Sciences Division, Earth System Research Laboratory, NOAA, Boulder, CO, USA

### Supporting Information:

Supporting Information may be found in the online version of this article.

### Correspondence to:

J. Quan and Y. Liu,  
[jqquan@ium.cn](mailto:jqquan@ium.cn);  
[liyuc@buct.edu.cn](mailto:liyuc@buct.edu.cn)

### Citation:

Ma, P., Quan, J., Dou, Y., Pan, Y., Liao, Z., Cheng, Z., et al. (2023). Regime-dependence of nocturnal nitrate formation via  $N_2O_5$  hydrolysis and its implication for mitigating nitrate pollution. *Geophysical Research Letters*, 50, e2023GL106183. <https://doi.org/10.1029/2023GL106183>

Received 5 SEP 2023  
 Accepted 18 NOV 2023

### Author Contributions:

**Conceptualization:** Jiannong Quan  
**Data curation:** Pengkun Ma, Yubing Pan, Xin Huang, Yongchun Liu  
**Formal analysis:** Pengkun Ma, Youjun Dou, Yubing Pan, Zhiheng Liao, Zhigang Cheng, Xingcan Jia, Qianqian Wang, Junlei Zhan, Wei Ma, Feixue Zheng, Yuzheng Wang, Yusheng Zhang, Chenjie Hua, Yongchun Liu  
**Investigation:** Pengkun Ma  
**Methodology:** Jiannong Quan, Yongchun Liu

**Abstract** The heterogeneous hydrolysis of dinitrogen pentoxide ( $N_2O_5$ ) is an important pathway in nitrate formation; however, its formation rate and relative contribution to total particulate nitrate ( $pNO_3^-$ ) are highly variable. Here we report that nocturnal  $pNO_3^-$  formation via  $N_2O_5$  hydrolysis is dependent on the regime defined by the ratio of  $NO_2$  to  $O_3$ . Nocturnal  $pNO_3^-$  formation via  $N_2O_5$  hydrolysis is suppressed in an  $O_3$ -limited regime but enhanced in a  $NO_2$ -limited regime. The results have crucial implications for effective control of nitrate pollution in the future. An exclusive decrease in  $NO_2$  will decrease nocturnal  $pNO_3^-$  formation in a  $NO_2$ -limited regime but may be less effective or even increase nocturnal  $pNO_3^-$  formation in an  $O_3$ -limited regime.

**Plain Language Summary** Our observations show that nocturnal  $pNO_3^-$  formation via dinitrogen pentoxide ( $N_2O_5$ ) hydrolysis in the residual layer over megacity Beijing is more efficient than at ground level. Further investigations suggest nocturnal  $pNO_3^-$  formation via  $N_2O_5$  hydrolysis is dependent on the regime defined by the ratio of  $NO_2$  to  $O_3$ . Nocturnal  $pNO_3^-$  formation via  $N_2O_5$  hydrolysis is suppressed in an  $O_3$ -limited regime but enhanced in a  $NO_2$ -limited regime. As a result, an exclusive decrease in  $NO_2$  will decrease nocturnal  $pNO_3^-$  formation in a  $NO_2$ -limited regime but may be less effective or even increase nocturnal  $pNO_3^-$  formation in an  $O_3$ -limited regime. The above result is also substantiated by observations during the COVID-19.

## 1. Introduction

Particulate nitrate ( $pNO_3^-$ ) is a major component of fine particles in urban regions (Baasandorj et al., 2017; Hoesly et al., 2018; McDuffie et al., 2019; Peng et al., 2021; Zheng et al., 2016). Nocturnal  $N_2O_5$  hydrolysis represents an important pathway of nitrate formation (Brown & Stutz, 2012; McDuffie et al., 2019; Seinfeld & Pandis, 2006; Zhang et al., 2015). Since the short lifetime of its precursor,  $NO_3$ , against photolysis and reaction with  $NO$  prevents buildup of appreciable  $N_2O_5$  mixing ratios during daytime (Brown et al., 2006), high  $N_2O_5$  mixing ratios and  $N_2O_5$  hydrolysis occur mainly at night. Compared to the relatively well-understood formation of nitrate via the gas-phase oxidation ( $OH + NO_2$ ), our understanding of  $N_2O_5$  hydrolysis remains elusive and the relative contribution from the  $N_2O_5$  hydrolysis on  $pNO_3^-$  is widely divergent in the literature, still lacking a comprehensive explanation. For example, some studies suggest that nocturnal heterogeneous chemistry outweighs the gas-phase oxidation pathway (Fan et al., 2021; Pathak et al., 2011; Prabhakar et al., 2017; Wang, Lu, et al., 2017; Yun et al., 2018), whereas others suggest that the gas-phase oxidation is dominant over the nocturnal  $N_2O_5$  hydrolysis reactions (Chen et al., 2020; Kuprov et al., 2014; Womack et al., 2019). These differences reflect in regional, seasonal, and even vertical aspects. For example, the relative contribution of  $N_2O_5$  hydrolysis reactions in summer and winter exhibit opposite trends in literature (Chen et al., 2020; Kenagy et al., 2018; Pathak et al., 2011). Furthermore, high concentrations of  $NO_3$  and  $N_2O_5$  in the residual layer (RL) are observed in some experiments (Wang et al., 2018; Yan et al., 2021), suggesting nocturnal nitrate formation in the RL may be

© 2023 The Authors.

This is an open access article under the terms of the [Creative Commons Attribution-NonCommercial License](https://creativecommons.org/licenses/by/4.0/), which permits use, distribution and reproduction in any medium, provided the original work is properly cited and is not used for commercial purposes.

**Software:** Pengkun Ma, Youjun Dou, Yubing Pan  
**Supervision:** Jiannong Quan  
**Validation:** Jiannong Quan  
**Writing – original draft:** Pengkun Ma, Jiannong Quan  
**Writing – review & editing:** Jiannong Quan, Chao Yan, Markku Kulmala, Yangang Liu, Xin Huang, Bin Yuan, Steven S. Brown, Yongchun Liu

enhanced despite low  $\text{NO}_x$  in this layer. The RL locates above the nocturnal stable boundary layer (SBL), which forms with radiative cooling of the ground after sunset.

$\text{N}_2\text{O}_5$  formation depends on both  $\text{NO}_x$  and  $\text{O}_3$ , while the latter is nonlinearly sensitive to  $\text{NO}_x$  and volatile organic compound (VOC) (Sillman & He, 2002). The  $\text{O}_3$  formation rate or yield may either increase or decrease with increasing  $\text{NO}_x$ , depending on the VOC concentration and composition. In a  $\text{NO}_x$ -limited regime of  $\text{O}_3$  formation, NO is oxidized dominantly by  $\text{HO}_2$  and  $\text{RO}_2$  to form  $\text{NO}_2$ , which then enhances  $\text{O}_3$  formation through photolysis (Atkinson, 2000; Sillman & West, 2009). Hence, an increase in NO emission will enhance both  $\text{NO}_2$  and  $\text{O}_3$ , which further enhances nocturnal  $\text{pNO}_3^-$  formation via  $\text{N}_2\text{O}_5$  hydrolysis. While in a VOC-limited regime, the consumption of radicals by excess  $\text{NO}_x$  limits  $\text{O}_3$  formation. Furthermore, photolytic production of radicals and  $\text{O}_3$  halts at night, and excess NO titrates the  $\text{O}_3$  to  $\text{NO}_2$ . As a result, an increase in NO emission enhances  $\text{NO}_2$  but decreases  $\text{O}_3$ , which may suppress nocturnal  $\text{pNO}_3^-$  formation. Therefore, the nocturnal  $\text{pNO}_3^-$  formation via  $\text{N}_2\text{O}_5$  hydrolysis may also be regime-dependent, affected by  $\text{O}_3$  formation sensitivity. In order to address this issue, the dependence of nocturnal  $\text{pNO}_3^-$  formation on its precursors is investigated in this work. We show, based on continuous observations and model simulations, that nocturnal  $\text{pNO}_3^-$  formation via  $\text{N}_2\text{O}_5$  hydrolysis can be divided into  $\text{NO}_2$ -limited,  $\text{O}_3$ -limited and transition regimes based on the ratio of  $\text{NO}_2$  to  $\text{O}_3$ , which is pertinent to understanding nocturnal  $\text{pNO}_3^-$  formation, and has crucial implications for mitigating  $\text{pNO}_3^-$  pollution.

## 2. Methods and Measurements

The comprehensive field campaign was conducted at the CITIC station and the BUCT station from October 17 to 12 November 2020. The BUCT station is located on the top floor of a five-story building (18 m above ground) with inlet lines going through the ceiling, which is used to represent observations near ground level, and the CITIC station is located on the roof of CITIC Tower with a height of 528 m above the ground. The measurements included aerosol composition ( $\text{SO}_4^{2-}$ ,  $\text{NO}_3^-$ ,  $\text{NH}_4^+$ ,  $\text{Cl}^-$ , and organic aerosols (OA)) by a Time-of-Flight aerosol chemical speciation monitor (ToF-ACSM), trace gases ( $\text{SO}_2$ ,  $\text{NO}_x$ , CO,  $\text{O}_3$ ), and meteorological variables. Radiosondes was used in boundary layer analysis, which was operated at the Guanxiangtai (GXT) meteorological station. To understand the dependence of  $\text{N}_2\text{O}_5$  on its precursors, observations of  $\text{N}_2\text{O}_5$  by a high-resolution Time-of-Flight chemical ionization mass spectrometer using iodide as the reagent ion (I-CIMS),  $\text{PM}_{2.5}$ , trace gases ( $\text{NO}_x$ ,  $\text{O}_3$ ), and meteorological variables were conducted at the BUCT station from 1 to 31 October 2021. The locations of the stations are illustrated in Figure S1 in Supporting Information S1 and the details of the measurements are described in Supporting Information S1. Observations from 17 October to 12 November 2020 at the CITIC station and the BUCT station are shown in Figure S2 in Supporting Information S1. Nitrogen chemistry and calculation of the formation rate of  $\text{pNO}_3^-$  through the  $\text{N}_2\text{O}_5$  heterogeneous reactions are described in Supporting Information S1.

## 3. Results and Discussion

### 3.1. Efficient Nocturnal $\text{pNO}_3^-$ Formation in the RL

The time series of  $\text{PM}_{2.5}$  chemical compositions,  $\text{NO}_x$ , and  $\text{O}_3$ , at the CITIC (China International Trust and Investment Corporation, 528 m above ground) and the BUCT (Beijing University of Chemical Technology, 18 m above ground) stations from 17 October to 12 November 2020, are shown in Figure S2 in Supporting Information S1. The observations indicated that nitrate was a dominant component in non-refractory  $\text{PM}_{2.5}$  (NR- $\text{PM}_{2.5}$ ) (Figures S2a and S2b in Supporting Information S1) at both the BUCT and CITIC stations. In polluted episodes, nitrate increased rapidly, with an increasing rate of  $0.3\text{--}2.4 \mu\text{g m}^{-3} \text{h}^{-1}$  at the BUCT station, and  $0.8\text{--}2.1 \mu\text{g m}^{-3} \text{h}^{-1}$  at the CITIC station. The mass fraction of nitrate in NR- $\text{PM}_{2.5}$  increased from  $17.8 \pm 10.2\%$  in clean episodes to  $40.8 \pm 11.7\%$  in polluted episodes at the CITIC station, and from  $24.7 \pm 11.8\%$  to  $45.1 \pm 10.2\%$  at the BUCT station, respectively. The clean and polluted groups are defined based on the  $\text{PM}_{2.5}$  mass concentration of  $<35 \mu\text{g m}^{-3}$  and  $\geq 35 \mu\text{g m}^{-3}$ , respectively. Although nitrate mass concentration at the CITIC station was consistent with that at the BUCT station, its precursor gases,  $\text{NO}_x$  ( $\text{NO} + \text{NO}_2$ ), at the CITIC station was much lower than that at the BUCT station (Figures S2c and S2d in Supporting Information S1), suggesting that the nitrate formation might be enhanced at the CITIC station. Moreover, striking differences existed in the diurnal variation of  $\text{pNO}_3^-$  and  $\text{NO}_x$  between the two stations (Figure 1). The mass concentration of  $\text{pNO}_3^-$  increased at night at the CITIC station with maximum  $\text{pNO}_3^-$  appeared in the early morning ( $11.0 \mu\text{g m}^{-3}$ , 04:00 LST), while at the

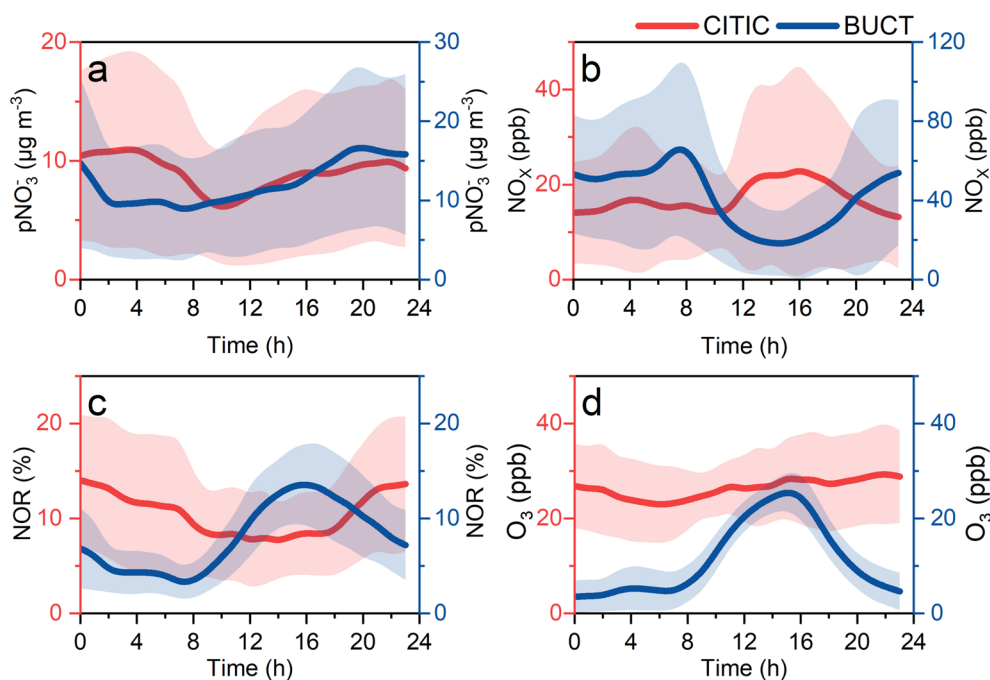


**Figure 1.** Diurnal variations of  $\text{pNO}_3^-$  mass concentrations,  $\text{NO}_x$ ,  $\text{O}_3$ , and NOR from October 17 to 12 November 2020, at the CITIC (red) and BUCT (blue) stations, respectively. The shaded areas denote standard deviation. The NOR is defined as the mole ratio of particle phase of nitrogen ( $\text{pNO}_3^-$ ) to total nitrogen (both  $\text{pNO}_3^-$  and  $\text{NO}_x$ ).

BUCT station  $\text{pNO}_3^-$  decreased at night with maximum  $\text{pNO}_3^-$  appeared at early night ( $16.7 \mu\text{g m}^{-3}$ , 20:00 LST). Conversely, the maximum  $\text{NO}_x$  appeared in the daytime at the CITIC station, but at night at the BUCT station. As a result, the maximum of the nitrogen oxidation ratio (NOR), that is, the mole ratio of particle phase of nitrogen ( $\text{pNO}_3^-$ ) to total nitrogen (both  $\text{pNO}_3^-$  and  $\text{NO}_x$ ), appeared at night at the CITIC station but in the daytime at the BUCT station. The averaged NOR during nighttime (18:00–06:00) was  $12.2 \pm 13.5\%$  at the CITIC, which was higher than that at the BUCT station ( $7.1 \pm 7.4\%$ ) by 70.9%. While in the daytime (07:00–17:00), the NOR at the CITIC ( $8.5 \pm 9.8\%$ ) was consistent with that at the BUCT station ( $9.0 \pm 7.7\%$ ). These observations substantiated that the nocturnal  $\text{pNO}_3^-$  production at the CITIC station was more efficient than at the BUCT station.

Combined analyses of boundary layer height and pollutants, indicate that vertical transport of pollutants from ground to the RL at night is significantly weakened. After sunset, the stable boundary layer (SBL) forms with radiative cooling of the ground and the daytime convective boundary layer (CBL) separates into SBL and RL (Stull, 1988). The decoupling between RL and SBL substantially weakens the vertical turbulent mixing of pollutants between the two layers. The RL largely maintains the atmospheric chemical state of the daytime CBL while the pollutants emitted near ground at night are trapped in the shallow SBL. An analysis of the boundary layer structure indicates that the CITIC station was located inside the RL at night while the BUCT station was located inside the SBL. The SBL height was usually lower than 300 m during the campaign based on radiosonde data at 08:00 and 20:00 LST (40 in 52 cases, Table S1 in Supporting Information S1). The contrary trends of  $\text{NO}_x$  in the CITIC and BUCT stations from 18:00 to 24:00 substantiated these analyses (Figure 1b). For example,  $\text{NO}_x$  increased at the BUCT station from  $27.1 \pm 27.1$  ppb to  $53.9 \pm 30.0$  ppb, but decreased from  $20.9 \pm 18.2$  ppb to  $13.2 \pm 10.7$  ppb at the CITIC station. The above analyses collectively indicate that high concentration of  $\text{pNO}_3^-$  in the RL at night is due mainly to efficient nocturnal  $\text{pNO}_3^-$  formation in the RL, rather than vertical transport from ground level, and it is important to investigate the mechanisms underlying this difference between the two layers.

### 3.2. Regimes in Nocturnal $\text{pNO}_3^-$ Formation

$\text{N}_2\text{O}_5$  hydrolysis is the dominant pathway of nocturnal  $\text{pNO}_3^-$  formation (Brown et al., 2006; Zhang et al., 2015). Primary emission of NO reacts with  $\text{HO}_2/\text{RO}_2/\text{O}_3$  to form  $\text{NO}_2$ . The reaction of  $\text{NO}_2$  with  $\text{O}_3$  produces the  $\text{NO}_3$  radical, which further reacts with  $\text{NO}_2$  to yield  $\text{N}_2\text{O}_5$  (Seinfeld & Pandis, 2006). The heterogeneous uptake of

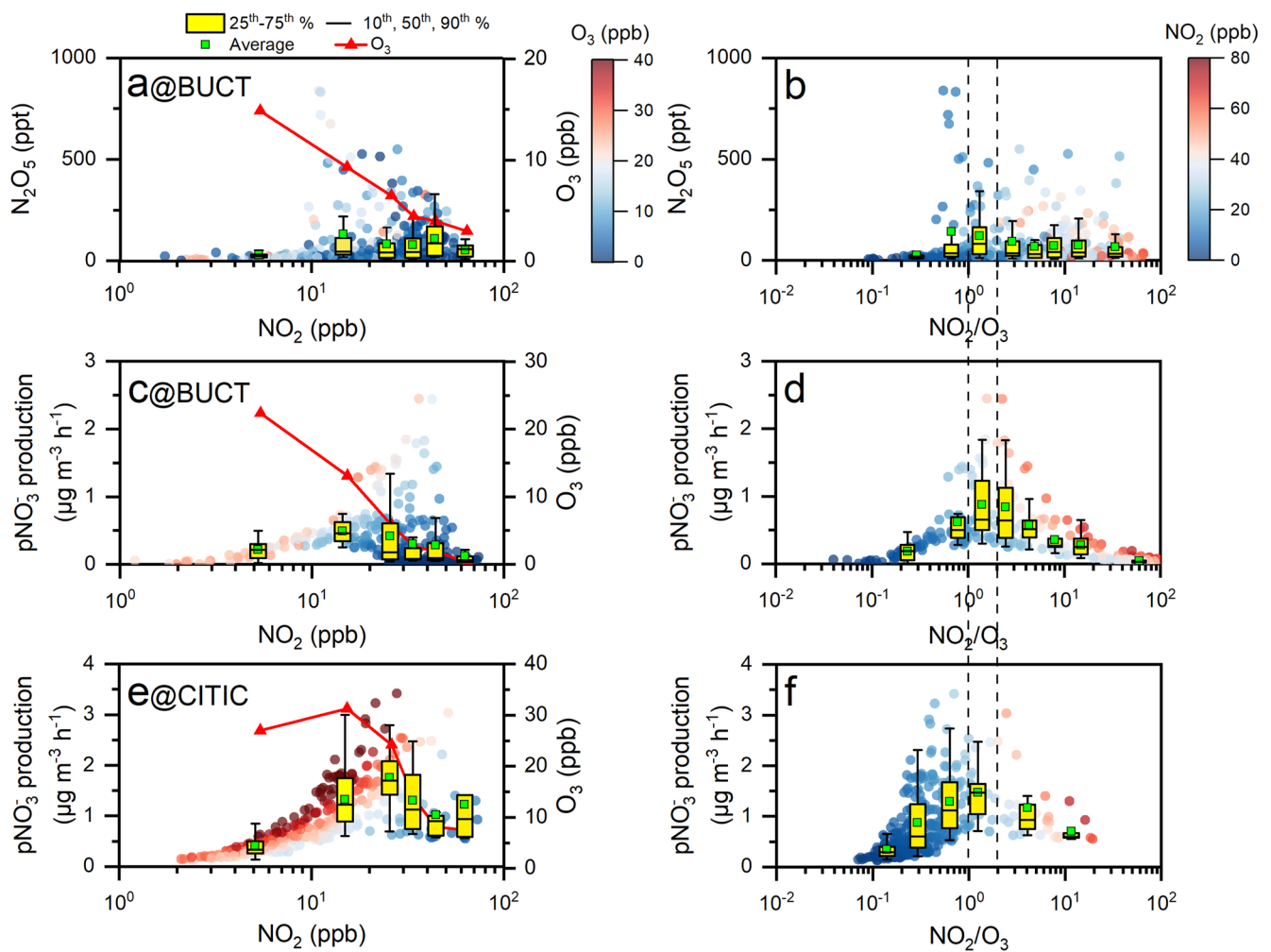


**Figure 2.** Relationships of the observed nocturnal  $N_2O_5$  to  $NO_2$  (a) and  $NO_2/O_3$  (b) at the BUCT station during 1–31 October 2021, and the simulated  $pNO_3^-$  via  $N_2O_5$  hydrolysis to  $NO_2$  (c, e) and  $NO_2/O_3$  (d, f) at the BUCT and CITIC stations, respectively, from 17 October to 12 November 2020. The dashed lines represent fixed value of  $NO_2/O_3$  of 1 and 2, respectively. Box and whisker plots show the 10th–90th percentile distributions of each bins, which are [0–10), [10–20), [20–30), [30–40), [40–50), [50–70) ppb for  $NO_2$  (a, c, e), and [0–0.5), [0.5–1), [1–2), [2–4), [4–6), [6–10), [10–20), [20–100) for  $NO_2/O_3$  (b, d, f). The red triangles show averaged  $O_3$  in each bin.

$N_2O_5$  on and within aerosol particles or fog/cloud droplets produces soluble nitrate. In spite of the well-known net reaction (i.e.,  $N_2O_5 + H_2O \rightarrow 2HNO_3$ ), the actual efficiency of  $N_2O_5$  hydrolysis is variable and difficult to quantify (McDuffie et al., 2018). This section investigates the complex relationships of nocturnal  $pNO_3^-$  formation to its precursors by both observations and model simulations.

The observational results show that the key nocturnal nitrogen species,  $N_2O_5$ , measured with an iodide-based chemical ionization mass spectrometer at the BUCT station on 1–31 October 2021 (see Methods and extended data shown in Figure S5 in Supporting Information S1), exhibited a nonlinear relationship with  $NO_2$ . The  $N_2O_5$ - $NO_x$  relationship exhibited a sign change from positive under low  $NO_2$  to negative under high  $NO_2$  concentration though with small fluctuations (Figure 2a).  $N_2O_5$  first increases with increasing  $NO_2$ , reaches its maximum when  $NO_2$  ranges from 10 to 20 ppb, and then decreases slightly with a further increase in  $NO_2$ , likely caused by decreased  $O_3$ . The relationship between  $N_2O_5$  and the ratio of  $NO_2$  to  $O_3$  ( $NO_2/O_3$ ) supports the above analyses, that is, high  $N_2O_5$  appears under a moderate  $NO_2/O_3$  (Figure 2b).

Simulations with a box model developed by Wagner et al. (2013) further support the observational result that the nocturnal formation rate of  $pNO_3^-$  is closely related to  $NO_2/O_3$  (Figures 2c–2f). Detailed description of the model and simulation setup is provided in Supporting Information S1. The simulations indicate that an increase in

$\text{NO}_2$  enhances nocturnal  $\text{pNO}_3^-$  formation under a fixed  $\text{O}_3$  level (Figures 2c and 2e). Whereas, nocturnal  $\text{pNO}_3^-$  formation is suppressed with a further increase in  $\text{NO}_2$  after the latter exceeds a certain threshold value, likely caused by a fast decrease in  $\text{O}_3$ . The relationship of nocturnal  $\text{pNO}_3^-$  formation rate to  $\text{NO}_2/\text{O}_3$  indicates that a maximum nocturnal  $\text{pNO}_3^-$  formation occurs in a moderate  $\text{NO}_2/\text{O}_3$ , ranging from 1 to 2, at both the CITIC and BUCT stations (Figures 2d and 2f).

Photochemical  $\text{O}_3$  production in Beijing near ground is often in a VOC-limited regime (Lu et al., 2010; Wang, Xue, et al., 2017). This means that high  $\text{NO}_x$  concentration strongly inhibits  $\text{O}_3$  formation. Recent observations indicate that the ratio of VOCs to  $\text{NO}_x$  increased with altitude (Tang et al., 2021), suggesting a change from a VOC-limited regime in  $\text{O}_3$  formation near ground to a  $\text{NO}_x$ -limited regime at higher elevation (Chen et al., 2020; Lu et al., 2010; Tang et al., 2021; Wagner et al., 2013; Wang et al., 2018). In our observations, the  $\text{O}_x$  ( $\text{NO}_2 + \text{O}_3$ ) are similar between CITIC and BUCT stations, but a high ratio of  $\text{NO}$  to  $\text{NO}_x$  (0.4–0.7) at night at the BUCT station, suggested that  $\text{NO}$  titration was mainly responsible for the sharp  $\text{O}_3$  drop near ground at night (Figure S7a in Supporting Information S1), resulting in a negative relationship between  $\text{O}_3$  and  $\text{NO}_x$  near ground (Figure S7b in Supporting Information S1). In a VOC-limited environment of  $\text{O}_3$  formation, the  $\text{O}_3$  near ground is very low at night due to  $\text{NO}_x$  suppression of  $\text{O}_3$  production during the previous day and  $\text{NO}$  titration at night. The averaged nocturnal (18:00–06:00)  $\text{O}_3$  was  $7.0 \pm 8.5$  ppb from 17 October to 12 November 2020. High  $\text{NO}_2$  ( $30.0 \pm 15.7$  ppb) and low  $\text{O}_3$  result in high  $\text{NO}_2/\text{O}_3$  (4.3). On the contrary, in the RL with a  $\text{NO}_x$ -limited environment, the nocturnal  $\text{NO}_2/\text{O}_3$  is much lower than that near ground. The averaged nocturnal  $\text{O}_3$  and  $\text{NO}_2$  were  $26.5 \pm 9.5$  and  $13.1 \pm 12.1$  ppb, respectively, with the  $\text{NO}_2/\text{O}_3$  of 0.49 during the same period. As a result, the modeled nocturnal  $\text{pNO}_3^-$  formation in the RL ( $0.82 \mu\text{g m}^{-3} \text{h}^{-1}$ ) was much higher than that near ground ( $0.28 \mu\text{g m}^{-3} \text{h}^{-1}$ ) though the nocturnal  $\text{NO}_2$  in the RL was much lower than that near ground. These analyses suggest that nocturnal  $\text{pNO}_3^-$  formation depends not only on its precursor ( $\text{NO}_x$ ) but also strongly on  $\text{NO}_2/\text{O}_3$ .

Based on R4 and R7 (in Supporting Information S1), one  $\text{O}_3$  molecule reacts with two  $\text{NO}_2$  molecules to form  $\text{N}_2\text{O}_5$ . Hence,  $\text{NO}_2$  will be in excess if the  $\text{NO}_2/\text{O}_3$  is higher than 2. The rate limiting step for this reaction (R4) is very slow. There is a separate, faster rate constant for titration of  $\text{O}_3$  by  $\text{NO}$  (R1), which occurs in a 1:1 ratio of  $\text{NO}_x$  and  $\text{O}_3$ . Thus the initial  $\text{O}_x$  partitioning between  $\text{NO}_2$  and  $\text{O}_3$  has a 1:1 stoichiometry, and  $\text{O}_3$  will be in excess if the ratio of  $\text{NO}_x$  (either emitted at the surface or remaining in the residual layer) to initial (late day)  $\text{O}_3$  is lower than 1. Hence, the  $\text{NO}_2/\text{O}_3$  of 1 and 2 can be used to identify whether  $\text{O}_3$  or  $\text{NO}_2$  is in excess, respectively, in  $\text{N}_2\text{O}_5$  and hence  $\text{pNO}_3^-$  formation, where values below 1 or above 2 result in  $\text{NO}_x$  or  $\text{O}_3$  limitations, respectively. The dependence of both observed  $\text{N}_2\text{O}_5$  and simulated  $\text{pNO}_3^-$  formation rate on  $\text{NO}_2/\text{O}_3$  supports the theoretical analyses. Efficient  $\text{pNO}_3^-$  formation will occur with a moderate  $\text{NO}_2/\text{O}_3$  ranging 1–2 (Figure 2). Based on the above analyses, the nocturnal  $\text{pNO}_3^-$  formation via  $\text{N}_2\text{O}_5$  hydrolysis is divided into three regimes based on  $\text{NO}_2/\text{O}_3$ : an  $\text{O}_3$ -limited regime ( $\text{NO}_2/\text{O}_3 > 2$ ), a  $\text{NO}_2$ -limited regime ( $\text{NO}_2/\text{O}_3 \leq 1$ ), and a transition regime ( $2 \geq \text{NO}_2/\text{O}_3 > 1$ ). We plot the relationship of modeled nocturnal  $\text{pNO}_3^-$  formation to  $\text{NO}_2$  and  $\text{O}_3$  based on data at the CITIC and BUCT stations from 17 October to 12 November 2020 (Figure 3), which clearly shows the regimes in nocturnal  $\text{pNO}_3^-$  formation. As analyzed above, nocturnal  $\text{pNO}_3^-$  formation at the BUCT station was in an  $\text{O}_3$ -limited regime from 17 October to 12 November 2020, with averaged nocturnal  $\text{NO}_2/\text{O}_3$  of 4.3. An increase in  $\text{NO}_2$  from  $22.4 \pm 11.4$  ppb in clean episodes to  $43.5 \pm 13.0$  ppb in polluted episodes, accompanied by a sharp decrease in  $\text{O}_3$  from  $8.8 \pm 8.8$  ppb to  $3.8 \pm 7.0$  ppb, results only in a slight increase in nocturnal  $\text{pNO}_3^-$  formation from  $0.27$  to  $0.31 \mu\text{g m}^{-3} \text{h}^{-1}$ , with the  $\Delta\text{pNO}_3^-/\Delta\text{NO}_2$  of  $0.0017 \mu\text{g m}^{-3} \text{h}^{-1} \text{ppb}^{-1}$ . On the other hand, nocturnal  $\text{pNO}_3^-$  formation at the CITIC station was in a  $\text{NO}_2$ -limited regime with averaged nocturnal  $\text{NO}_2/\text{O}_3$  of 0.49 during the same period. An increase in  $\text{NO}_2$  from  $7.4 \pm 4.4$  ppb in clean episodes to  $23.3 \pm 14.7$  ppb in polluted episodes, accompanied by a slight increase in  $\text{O}_3$  from  $26.1 \pm 5.7$  to  $27.0 \pm 13.8$  ppb, results in a significant increase in nocturnal  $\text{pNO}_3^-$  formation from  $0.51$  to  $1.36 \mu\text{g m}^{-3} \text{h}^{-1}$  (Figure 3), with the  $\Delta\text{pNO}_3^-/\Delta\text{NO}_2$  of  $0.053 \mu\text{g m}^{-3} \text{h}^{-1} \text{ppb}^{-1}$ . These analyses indicate that the nocturnal  $\text{pNO}_3^-$  formation strongly depends on the regimes as defined by  $\text{NO}_2/\text{O}_3$ ; nocturnal  $\text{pNO}_3^-$  formation is suppressed in the  $\text{O}_3$ -limited regime while enhanced in the  $\text{NO}_2$ -limited regime. Sensitivity analysis further reveals that nocturnal  $\text{pNO}_3^-$  formation near ground will increase from  $0.28$  to  $1.9 \mu\text{g m}^{-3} \text{h}^{-1}$  if the corresponding  $\text{O}_3$  increases from  $7.0$  to  $26.2$  ppb, same as in the RL, while other pollutants (e.g.,  $\text{NO}_x$  and  $\text{PM}_{2.5}$ ) and meteorological variables (e.g., T and RH) remain unchanged, further confirming that the nocturnal  $\text{pNO}_3^-$  formation at ground level is strongly suppressed in an  $\text{O}_3$ -limited environment.

To understand the relative contribution of  $\text{N}_2\text{O}_5$  hydrolysis to  $\text{pNO}_3^-$  formation, we also simulate the  $\text{pNO}_3^-$  formation via gas-phase oxidation ( $\text{OH} + \text{NO}_2$ ) (see Supporting Information S1). The result indicates that the

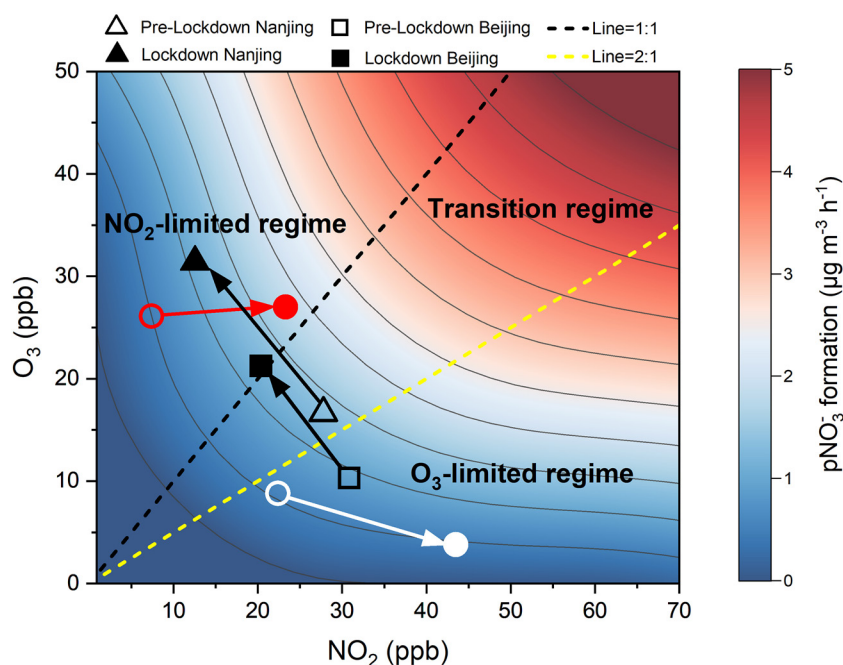


**Figure 3.** Sensitivity of the  $\text{pNO}_3^-$  formation via  $\text{N}_2\text{O}_5$  hydrolysis to  $\text{O}_3$  and  $\text{NO}_2$ , with the data at CITIC and BUCT from 17 October to 12 November 2020 (same as Figures 2c–2f). The red and white circles represent averaged  $\text{O}_3$  and  $\text{NO}_2$  at the CITIC and BUCT stations in clean (hollow) and polluted episodes (solid), respectively. The hollow and solid squares represent Beijing during Pre-lockdown and Lockdown, and the hollow and solid triangles represent Nanjing during Pre-lockdown and Lockdown.

rate of  $\text{pNO}_3^-$  formation via gas-phase oxidation between the two stations was very similar (with averaged 1.43 and 1.45  $\mu\text{g m}^{-3} \text{h}^{-1}$  at the CITIC and BUCT station for the entire study period, respectively), suggesting that the  $\text{N}_2\text{O}_5$  hydrolysis contributes 40.5% in total nitrate formation at the CITIC station from 17 October to 12 November 2020, which was much higher than the 18.9% at the BUCT station. Such differences were more evident in polluted episodes than in clean episodes. In clean episodes, the  $\text{N}_2\text{O}_5$  hydrolysis contributed 18.1% and 29.5% in total nitrate formation at the BUCT and CITIC stations, respectively; while in polluted episodes its contribution was 20.3% and 54.2% at the BUCT and CITIC stations, respectively. The  $\text{NO}_2$ -limited regime in the RL favors efficient nocturnal  $\text{pNO}_3^-$  formation, which well explained the higher nocturnal NOR in the RL in observations, rather than near ground (Figure 1c). In the calculation, the steady-state assumption of  $\text{NO}_3$  and  $\text{N}_2\text{O}_5$  may not hold if there is strong  $\text{NO}$  emission nearby, especially at ground level with large on-road traffic volume. While in the residual layer,  $\text{NO}_3$  and  $\text{N}_2\text{O}_5$  were likely in a steady state since there has not fresh  $\text{NO}$  emission the residual layer. As a result, the calculation of nocturnal nitrate formation in the residual layer is less affected while the calculation at ground level may be overestimated.

The different regimes between the ground level and RL influence the overall vertical distribution of  $\text{pNO}_3^-$  and other pollutants. Also influence the vertical transport of nitrate and its precursors. The weakened nocturnal  $\text{pNO}_3^-$  formation at ground due to  $\text{O}_3$ -limited regime may enhance  $\text{NO}_x$  accumulation at night. As a result, more  $\text{NO}_x$  is upwards transported to high layer next morning and stores in the RL, where  $\text{NO}_x$  is converted to  $\text{pNO}_3^-$  efficiently via  $\text{N}_2\text{O}_5$  hydrolysis at night. The  $\text{pNO}_3^-$  formed in the RL at night may be entrained downward to ground level in the following morning through convective mixing and deteriorates air pollution near the ground (Pathak et al., 2011). Hence, the nocturnal  $\text{pNO}_3^-$  formation in the RL is an important source of  $\text{pNO}_3^-$  and should be considered in evaluating the source of  $\text{pNO}_3^-$  in the troposphere, including at surface level.

### 3.3. Implication for Future $\text{pNO}_3^-$ Control

An analysis of the ratio of nocturnal  $\text{NO}_2$  to  $\text{O}_3$  in China, based on observations at 2024 stations during 2015–2021 (CNEMC, 2023), shows that the regime of nocturnal  $\text{pNO}_3^-$  formation exhibits obvious regional and seasonal variations (Figure S8 in Supporting Information S1). In summer and spring, most regions in China lies in the

$\text{NO}_2$ -limited regime; while the situation is more complicated in autumn and winter, with some regions (e.g., North China Plain (NCP), Guanzhong Basin, and Chengdu-Chongqing Zone) transitioning to the  $\text{O}_3$ -limited regime. Such regime variations well explain the variations in nocturnal nitrate formation rate via  $\text{N}_2\text{O}_5$  hydrolysis estimated in previous studies for different regions and seasons, for example, higher formation rate in south China (Yang et al., 2022; Yun et al., 2018) than north China (Chen et al., 2020), in summer (Pathak et al., 2011; Tan et al., 2021) than in winter (Chen et al., 2020). This general explainability further reinforces our proposal that nocturnal  $\text{pNO}_3^-$  formation via  $\text{N}_2\text{O}_5$  hydrolysis is highly regime-dependent.

Reducing  $\text{NO}_x$  emission from traffic sectors has long been considered as a normal protocol in implementing regulatory policies (Guo et al., 2016). Based on this study, the nocturnal  $\text{pNO}_3^-$  formation via  $\text{N}_2\text{O}_5$  hydrolysis depends strongly on the regimes as defined by the ratio of  $\text{NO}_2$  to  $\text{O}_3$ . Hence, the regime behavior should be considered in  $\text{pNO}_3^-$  control. The outbreak of COVID-19 provides an exceptionally unique opportunity to assess the responses of nitrate chemistry to  $\text{NO}_x$  reduction under different regimes. To control the COVID-19 pandemic, a lockdown was imposed, during which a dramatic reduction in  $\text{NO}_x$  concentration was observed worldwide (Cooper et al., 2022; Miyazaki et al., 2021; Shi et al., 2021; Venter et al., 2020). In China,  $\text{NO}_x$  concentration decreased by up to 93% during the Lockdown period (Huang & Sun, 2020; Le et al., 2020; Shi & Brasseur, 2020). However, such a sharp decrease in  $\text{NO}_x$  did not result in a clear decrease in  $\text{PM}_{2.5}$ . A possible explanation is that a decrease in  $\text{NO}_x$  resulted in  $\text{O}_3$  enhancement, which strengthened the atmospheric oxidizing capacity and facilitated secondary aerosol formation (Huang et al., 2021; Le et al., 2020; Li et al., 2022). Even more surprising is that both the mass concentration of nitrate and its mass fraction in  $\text{PM}_{2.5}$  during the Lockdown period exhibited opposite changes between south and north China despite similar sharp decrease in  $\text{NO}_x$  emission, an increase in north China (e.g. Beijing) but a decrease in south China (e.g. Nanjing) (Ren et al., 2021).

To understand the regime effect on nitrate control, nocturnal  $\text{pNO}_3^-$  formation during Pre-Lockdown (1 to 22 January 2020) and Lockdown period (23 January to 15 February 2020) is also simulated with the box model developed by Wagner et al. (2013) (Figure 4). As shown in Figure S8 in Supporting Information S1, nocturnal  $\text{pNO}_3^-$  formation in north China is under an  $\text{O}_3$ -limited regime in winter, but under  $\text{NO}_2$ -limited or transition regime in south China. Beijing and Nanjing are selected to represent north and south China, respectively. The nocturnal  $\text{NO}_2/\text{O}_3$  were 3.0 and 1.7 at Beijing and Nanjing, respectively, during the Pre-lockdown, indicating a typical  $\text{O}_3$ -limited regime at Beijing, but a transition regime at Nanjing. Nocturnal  $\text{NO}_x$  in Beijing decreased from  $51.1 \pm 42.2$  ppb during the Pre-Lockdown to  $21.5 \pm 14.7$  ppb during the Lockdown, among which NO decreased sharply from  $20.3 \pm 32.4$  to  $1.2 \pm 3.0$  ppb with a decreasing rate of 94.3%, indicating that  $\text{O}_3$  depletion due to NO titration was sharply weakened during the Lockdown. As a result,  $\text{O}_3$  increased from  $10.3 \pm 11.1$  to  $21.3 \pm 13.1$  ppb and the  $\text{NO}_2/\text{O}_3$  decreased to 0.96 during the Lockdown, suggesting a conversion from  $\text{O}_3$ -limited regime during the Pre-Lockdown to  $\text{NO}_2$ -limited regime during the Lockdown. As a result, the nocturnal  $\text{pNO}_3^-$  formation via  $\text{N}_2\text{O}_5$  hydrolysis increased from  $0.37 \mu\text{g m}^{-3} \text{h}^{-1}$  during the Pre-Lockdown to  $0.74 \mu\text{g m}^{-3} \text{h}^{-1}$  during the Lockdown though  $\text{NO}_x$  decreased by 56.1%. By contrast, nocturnal  $\text{NO}_x$  in Nanjing decreased from  $34.5 \pm 23.7$  ppb during the Pre-Lockdown to  $12.9 \pm 6.9$  ppb during the Lockdown, among which NO also decreased sharply from  $6.7 \pm 17.1$  ppb to  $0.36 \pm 1.8$  ppb. As a result,  $\text{O}_3$  increased from  $16.6 \pm 13.3$  ppb to  $31.4 \pm 13.0$  ppb and the  $\text{NO}_2/\text{O}_3$  further decreased to 0.4 during the Lockdown, suggesting a conversion from transition regime during the Pre-Lockdown to  $\text{NO}_2$ -limited regime. Contrary to Beijing, the nocturnal  $\text{pNO}_3^-$  formation in Nanjing decreased from  $0.90 \mu\text{g m}^{-3} \text{h}^{-1}$  during the Pre-Lockdown to  $0.78 \mu\text{g m}^{-3} \text{h}^{-1}$  during the Lockdown, with a decreasing rate of 13.2%. The above results are consistent with the opposite trends of  $\text{pNO}_3^-$  mass concentration from the Pre-Lockdown to the Lockdown in the two cities in observations (Ren et al., 2021). The contrary trends in nocturnal  $\text{pNO}_3^-$  formation between Beijing and Nanjing under similar  $\text{NO}_x$  decrease confirm the analysis in this paper that the nocturnal  $\text{pNO}_3^-$  formation is strongly regime-dependent; a decrease in  $\text{NO}_2$  will decrease nocturnal  $\text{pNO}_3^-$  in a  $\text{NO}_2$ -limited or transition regime, but will be less effective or even increase nocturnal  $\text{pNO}_3^-$  in an  $\text{O}_3$ -limited regime (Figure 3). It is noteworthy that only nocturnal  $\text{pNO}_3^-$  formation via  $\text{N}_2\text{O}_5$  hydrolysis in response to changing  $\text{NO}_x$  emissions were investigated in this work, while daytime nitrate formation, gas-particle partitioning, and particulate nitrate lifetime also need to be considered when determining how particulate nitrate concentrations would change in response to changing emissions (Zhai et al., 2021).

#### 4. Summary

Nitrate is a major component of fine particles in cities and mitigation strategies have been normally focused on  $\text{NO}_x$  control. This study suggests that nocturnal  $\text{pNO}_3^-$  formation via  $\text{N}_2\text{O}_5$  hydrolysis depends on the regime

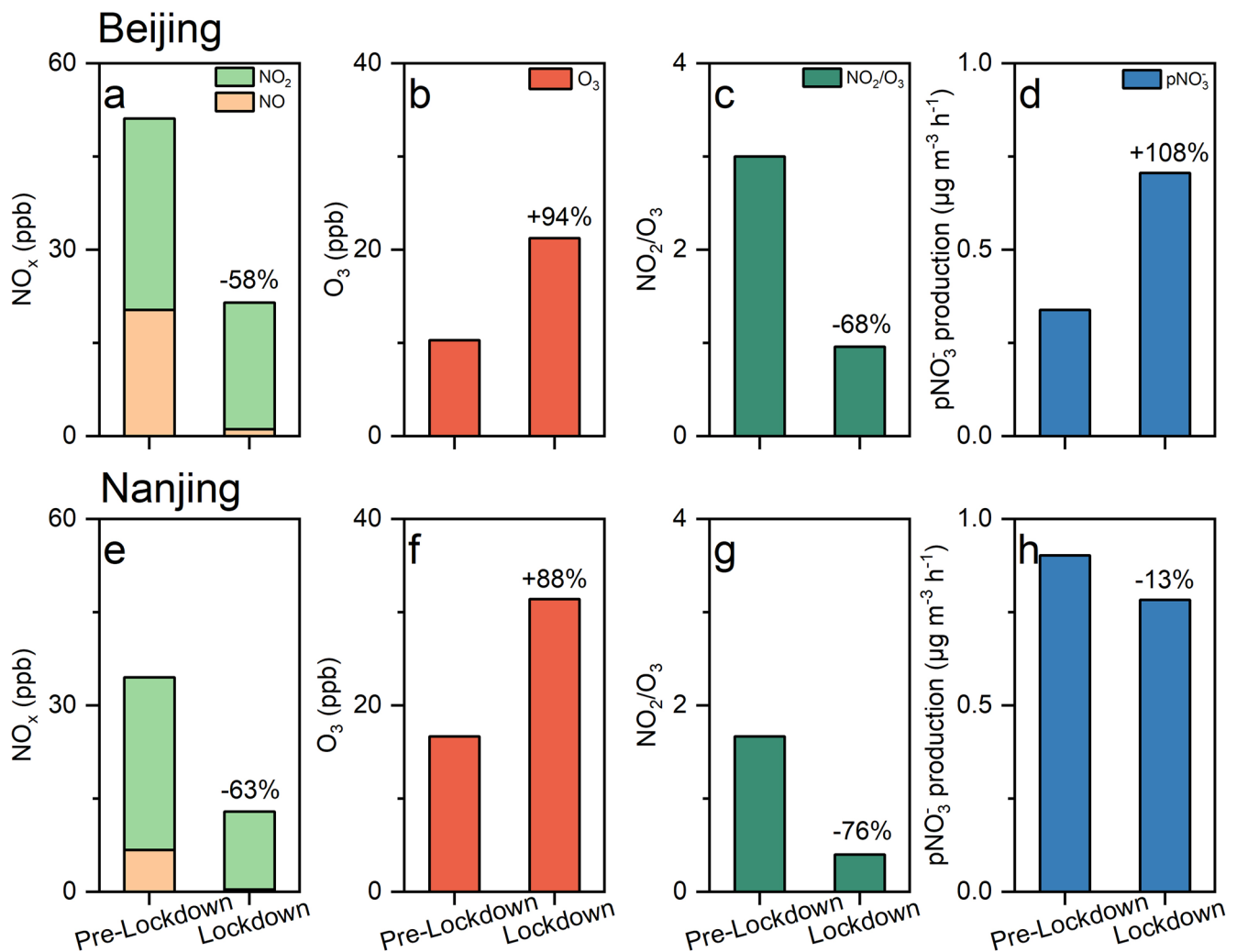


**Figure 4.** Variations in  $\text{NO}_x$ ,  $\text{O}_3$ ,  $\text{NO}_2/\text{O}_3$ , and  $\text{pNO}_3^-$  formation via  $\text{N}_2\text{O}_5$  hydrolysis in Beijing (upper panel) and Nanjing (bottom panel) during the Lockdown and Pre-Lockdown, respectively.

as defined by the ratio of  $\text{NO}_2$  to  $\text{O}_3$ . A  $\text{NO}_2$ -limited regime in the RL favors nocturnal  $\text{pNO}_3^-$  formation while an  $\text{O}_3$ -limited regime at ground level suppresses nocturnal  $\text{pNO}_3^-$  formation. As a result, more  $\text{NO}_x$  is upwards transported in the daytime and converted to  $\text{pNO}_3^-$  efficiently via  $\text{N}_2\text{O}_5$  hydrolysis at night in the RL. Hence, the nocturnal  $\text{pNO}_3^-$  formation in the RL is an important source of  $\text{pNO}_3^-$  and should be considered in evaluating the source of  $\text{pNO}_3^-$  in the troposphere, including at surface level. Regime-dependence of nocturnal nitrate formation has crucial implications for effective control of nitrate pollution. A reduction in  $\text{NO}_x$  alone can only reduce nocturnal  $\text{pNO}_3^-$  formation when the atmosphere is in the  $\text{NO}_2$ -limited regime; it becomes less effective or may even enhance nocturnal  $\text{pNO}_3^-$  when the atmosphere is in the  $\text{O}_3$ -limited regime. Therefore, a more comprehensive regulation of precursor gases (e.g., VOCs and  $\text{NO}_x$ ) is needed when developing an emission control strategy to mitigate nitrate pollution.

### Conflict of Interest

The authors declare no conflicts of interest relevant to this study.

### Data Availability Statement

Data are available through Quan (2023).



**Acknowledgments**

This research is supported by Chinese Key Projects in the National Science and Technology (2023YFC3711000, 2017YFC0209604) and the National Natural Science Foundation of China (42275117). Y.L. is supported by the US Department of Energy's Atmospheric System Research (ASR) Program.

**References**

Atkinson, R. (2000). Atmospheric chemistry of VOCs and NO<sub>x</sub>. *Atmospheric Environment*, 34(12–14), 2063–2101. [https://doi.org/10.1016/S1352-2310\(99\)00460-4](https://doi.org/10.1016/S1352-2310(99)00460-4)

Baasandorj, M., Hoch, S. W., Bares, R., Lin, J. C., Brown, S. S., Millet, D. B., et al. (2017). Coupling between chemical and meteorological processes under persistent cold-air pool conditions: Evolution of wintertime PM<sub>2.5</sub> pollution events and N<sub>2</sub>O<sub>5</sub> observations in Utah's Salt Lake Valley. *Environmental Science & Technology*, 51(11), 5941–5950. <https://doi.org/10.1021/acs.est.6b06603>

Brown, S. S., Ryerson, T. B., Wollny, A. G., Brock, C. A., Peltier, R., Sullivan, A. P., et al. (2006). Variability in nocturnal nitrogen oxide processing and its role in regional air quality. *Science*, 311(5757), 67–70. <https://doi.org/10.1126/science.1120120>

Brown, S. S., & Stutz, J. (2012). Nighttime radical observations and chemistry. *Chemical Society Reviews*, 41(19), 6405–6447. <https://doi.org/10.1039/c2cs35181a>

Chen, X. R., Wang, H. C., Lu, K. D., Li, C. M., Zhai, T. Y., Tan, Z. F., et al. (2020). Field determination of nitrate formation pathway in winter Beijing. *Environmental Science & Technology*, 54(15), 9243–9253. <https://doi.org/10.1021/acs.est.0c00972>

CNEMC. (2023). Observations of NO<sub>2</sub> and O<sub>3</sub> in China during 2015–2021. Retrieved from <http://www.cnemc.cn/>

Cooper, M. J., Martin, R. V., Hammer, M. S., Levelt, P. F., Veefkind, P., Lamsal, L. N., et al. (2022). Global fine-scale changes in ambient NO<sub>2</sub> during COVID-19 lockdowns. *Nature*, 601(7893), 380–387. <https://doi.org/10.1038/s41586-021-04229-0>

Fan, M. Y., Zhang, Y. L., Lin, Y. C., Hong, Y., Zhao, Z. Y., Xie, F., et al. (2021). Important role of NO<sub>3</sub> radical to nitrate formation aloft in urban Beijing: Insights from triple oxygen isotopes measured at the tower. *Environmental Science & Technology*, 11, 6870–6879. <https://doi.org/10.1021/acs.est.1c02843>

Guo, X. R., Fu, L. W., Ji, M. S., Lang, J. L., Chen, D. S., & Cheng, S. Y. (2016). Scenario analysis to vehicular emission reduction in Beijing-Tianjin-Hebei (BTH) region, China. *Environmental Pollution*, 216, 470–479. <https://doi.org/10.1016/j.envpol.2016.05.082>

Hoesly, R. M., Smith, S. J., Feng, L. Y., Klimont, Z., Janssens-Maenhout, G., Pitkanen, T., et al. (2018). Historical (1750–2014) anthropogenic emissions of reactive gases and aerosols from the Community Emissions Data System (CEDS) (p. 11).

Huang, G. Y., & Sun, K. (2020). Non-negligible impacts of clean air regulations on the reduction of tropospheric NO<sub>2</sub> over East China during the COVID-19 pandemic observed by OMI and TROPOMI. *Science of the Total Environment*, 745.

Huang, X., Ding, A. J., Gao, J., Zheng, B., Zhou, D. R., Qi, X. M., et al. (2021). Enhanced secondary pollution offset reduction of primary emissions during COVID-19 lockdown in China. *National Science Review*, 8(2). <https://doi.org/10.1093/nsr/nwaa137>

Kenagy, H. S., Sparks, T. L., Ebben, C. J., Wooldrige, P. J., Lopez-Hilfiker, F. D., Lee, B. H., et al. (2018). NO<sub>x</sub> lifetime and NO<sub>y</sub> partitioning during WINTER. *Journal of Geophysical Research: Atmospheres*, 123(17), 9813–9827. <https://doi.org/10.1029/2018jd028736>

Kuprov, R., Eatough, D. J., Cruickshank, T., Olson, N., Cropper, P. M., & Hansen, J. C. (2014). Composition and secondary formation of fine particulate matter in the Salt Lake Valley: Winter 2009. *Journal of the Air & Waste Management Association*, 64(8), 957–969. <https://doi.org/10.1080/10962247.2014.903878>

Le, T. H., Wang, Y., Liu, L., Yang, J. N., Yung, Y. L., Li, G. H., & Seinfeld, J. H. (2020). Unexpected air pollution with marked emission reductions during the COVID-19 outbreak in China. *Science*, 369(6504), 702–706. <https://doi.org/10.1126/science.abb7431>

Li, X., Bei, N. F., Wu, J. R., Liu, S. X., Wang, Q. Y., Tian, J., et al. (2022). The heavy particulate matter pollution during the COVID-19 lockdown period in the Guanzhong Basin, China. *Journal of Geophysical Research: Atmospheres*, 127(8), e2021JD036191. <https://doi.org/10.1029/2021jd036191>

Lu, K. D., Zhang, Y. H., Su, H., Brauers, T., Chou, C. C., Hofzumahaus, A., et al. (2010). Oxidant (O<sub>3</sub> + NO<sub>2</sub>) production processes and formation regimes in Beijing. *Journal of Geophysical Research*, 115(D7), D07303. <https://doi.org/10.1029/2009jd012714>

McDuffie, E. E., Fibiger, D. L., Dube, W. P., Lopez-Hilfiker, F., Lee, B. H., Thornton, J. A., et al. (2018). Heterogeneous N<sub>2</sub>O<sub>5</sub> uptake during winter: Aircraft measurements during the 2015 WINTER campaign and critical evaluation of current parameterizations. *Journal of Geophysical Research: Atmospheres*, 123(8), 4345–4372. <https://doi.org/10.1002/2018jd028336>

McDuffie, E. E., Womack, C. C., Fibiger, D. L., Dube, W. P., Franchin, A., Middlebrook, A. M., et al. (2019). On the contribution of nocturnal heterogeneous reactive nitrogen chemistry to particulate matter formation during wintertime pollution events in Northern Utah. *Atmospheric Chemistry and Physics*, 19(14), 9287–9308. <https://doi.org/10.5194/acp-19-9287-2019>

Miyazaki, K., Bowman, K., Sekiya, T., Takigawa, M., Neu, J. L., Sudo, K., et al. (2021). Global tropospheric ozone responses to reduced NO<sub>x</sub> emissions linked to the COVID-19 worldwide lockdowns. *Science Advances*, 7(24). <https://doi.org/10.1126/sciadv.abf7460>

Pathak, R. K., Wang, T., & Wu, W. S. (2011). Nighttime enhancement of PM<sub>2.5</sub> nitrate in ammonia-poor atmospheric conditions in Beijing and Shanghai: Plausible contributions of heterogeneous hydrolysis of N<sub>2</sub>O<sub>5</sub> and HNO<sub>3</sub> partitioning. *Atmospheric Environment*, 45(5), 1183–1191. <https://doi.org/10.1016/j.atmosenv.2010.09.003>

Peng, J., Hu, M., Shang, D., Wu, Z., Du, Z., Tan, T., et al. (2021). Explosive secondary aerosol formation during severe haze in the North China Plain. *Environmental Science & Technology*, 55(4), 2189–2207. <https://doi.org/10.1021/acs.est.0c07204>

Prabhakar, G., Parworth, C. L., Zhang, X., Kim, H., Young, D. E., Beyersdorf, A. J., et al. (2017). Observational assessment of the role of nocturnal residual-layer chemistry in determining daytime surface particulate nitrate concentrations. *Atmospheric Chemistry and Physics*, 17(23), 14747–14770. <https://doi.org/10.5194/acp-17-14747-2017>

Quan, J. N. (2023). Regime-dependence of nocturnal nitrate formation via N<sub>2</sub>O<sub>5</sub> hydrolysis and its implication for mitigating nitrate pollution [Dataset]. Zenodo. <https://zenodo.org/record/8320463>

Ren, C. H., Huang, X., Wang, Z. L., Sun, P., Chi, X. G., Ma, Y., et al. (2021). *Nonlinear response of nitrate to NOx reduction in China during the COVID-19 pandemic* (p. 264). Atmospheric Environment.

Seinfeld, J. H., & Pandis, S. N. (2006). *Atmospheric chemistry and physics: From air pollution to climate change* 2nd ed.

Shi, X. Q., & Brasseur, G. P. (2020). The response in air quality to the reduction of Chinese economic activities during the COVID-19 outbreak. *Geophysical Research Letters*, 47(11), e2020GL088070. <https://doi.org/10.1029/2020gl088070>

Shi, Z. B., Song, C. B., Liu, B. W., Lu, G. D., Xu, J. S., Vu, T. V., et al. (2021). Abrupt but smaller than expected changes in surface air quality attributable to COVID-19 lockdowns. *Science Advances*, 7(3). <https://doi.org/10.1126/sciadv.abd6696>

Sillman, S., & He, D. Y. (2002). Some theoretical results concerning O<sub>3</sub>-NO<sub>x</sub>-VOC chemistry and NO<sub>x</sub>-VOC indicators. *Journal of Geophysical Research*, 107(D22), ACH26-1–ACH26-15. <https://doi.org/10.1029/2001jd001123>

Sillman, S., & West, J. J. (2009). Reactive nitrogen in Mexico City and its relation to ozone-precursor sensitivity: Results from photochemical models. *Atmospheric Chemistry and Physics*, 9(11), 3477–3489. <https://doi.org/10.5194/acp-9-3477-2009>

Stull, R. B. (1988). *An introduction to boundary layer meteorology*. Springer Netherlands.

Tan, Z., Wang, H. C., Lu, K. D., Dong, H. B., Liu, Y. H., Zeng, L. M., et al. (2021). An observational based modeling of the surface layer particulate nitrate in the north China plain during summertime. *Journal of Geophysical Research: Atmospheres*, 126(18), e2021JD035623. <https://doi.org/10.1029/2021jd035623>

- Tang, G. Q., Wang, Y. H., Liu, Y. S., Wu, S., Huang, X. J., Yang, Y., et al. (2021). Low particulate nitrate in the residual layer in autumn over the North China Plain. *Science of the Total Environment*, 782, 146845. <https://doi.org/10.1016/j.scitotenv.2021.146845>
- Venter, Z. S., Aunan, K., Chowdhury, S., & Lelieveld, J. (2020). COVID-19 lockdowns cause global air pollution declines. *Proceedings of the National Academy of Sciences of the United States of America*, 117(32), 18984–18990. <https://doi.org/10.1073/pnas.2006853117>
- Wagner, N. L., Riedel, T. P., Young, C. J., Bahreini, R., Brock, C. A., Dube, W. P., et al. (2013). N<sub>2</sub>O<sub>5</sub> uptake coefficients and nocturnal NO<sub>2</sub> removal rates determined from ambient wintertime measurements. *Journal of Geophysical Research-Atmospheres*, 118(16), 9331–9350. <https://doi.org/10.1002/jgrd.50653>
- Wang, H. C., Lu, K. D., Chen, X. R., Zhu, Q. D., Chen, Q., Guo, S., et al. (2017). High N<sub>2</sub>O<sub>5</sub> concentrations observed in urban Beijing: Implications of a large nitrate formation pathway. *Environmental Science and Technology Letters*, 4(10), 416–420. <https://doi.org/10.1021/acs.estlett.7b00341>
- Wang, H. C., Lu, K. D., Chen, X. R., Zhu, Q. D., Wu, Z. J., Wu, Y. S., & Sun, K. (2018). Fast particulate nitrate formation via N<sub>2</sub>O<sub>5</sub> uptake aloft in winter in Beijing. *Atmospheric Chemistry and Physics*, 18(14), 10483–10495. <https://doi.org/10.5194/acp-18-10483-2018>
- Wang, T., Xue, L., Brimblecombe, P., Lam, Y. F., Li, L., & Zhang, L. (2017). Ozone pollution in China: A review of concentrations, meteorological influences, chemical precursors, and effects. *Science of the Total Environment*, 575, 1582–1596. <https://doi.org/10.1016/j.scitotenv.2016.10.081>
- Womack, C. C., McDuffie, E. E., Edwards, P. M., Bares, R., de Gouw, J. A., Docherty, K. S., et al. (2019). An odd oxygen framework for wintertime ammonium nitrate aerosol pollution in urban areas: NO<sub>x</sub> and VOC control as mitigation strategies. *Geophysical Research Letters*, 46(9), 4971–4979. <https://doi.org/10.1029/2019gl082028>
- Yan, Y. H., Wang, S. S., Zhu, J., Guo, Y. L., Tang, G. Q., Liu, B. X., et al. (2021). Vertically increased NO<sub>3</sub> radical in the nocturnal boundary layer. *Science of the Total Environment*, 763.
- Yang, S., Yuan, B., Peng, Y., Huang, S., Chen, W., Hu, W., et al. (2022). The formation and mitigation of nitrate pollution: Comparison between urban and suburban environments. *Atmospheric Chemistry and Physics*, 22(7), 4539–4556. <https://doi.org/10.5194/acp-22-4539-2022>
- Yun, H., Wang, W., Wang, T., Xia, M., Yu, C., Wang, Z., et al. (2018). Nitrate formation from heterogeneous uptake of dinitrogen pentoxide during a severe winter haze in southern China. *Atmospheric Chemistry and Physics*, 18(23), 17515–17527. <https://doi.org/10.5194/acp-18-17515-2018>
- Zhai, S., Jacob, D. J., Wang, X., Liu, Z., Wen, T., Shah, V., et al. (2021). Control of particulate nitrate air pollution in China. *Nature Geoscience*, 14(6), 389–395. <https://doi.org/10.1038/s41561-021-00726-z>
- Zhang, R. Y., Wang, G. H., Guo, S., Zamora, M. L., Ying, Q., Lin, Y., et al. (2015). Formation of urban fine particulate matter. *Chemical Reviews*, 115(10), 3803–3855. <https://doi.org/10.1021/acs.chemrev.5b00067>
- Zheng, J., Hu, M., Peng, J., Wu, Z., Kumar, P., Li, M., et al. (2016). Spatial distributions and chemical properties of PM<sub>2.5</sub> based on 21 field campaigns at 17 sites in China. *Chemosphere*, 159, 480–487. <https://doi.org/10.1016/j.chemosphere.2016.06.032>